A Loop Deletion in the Plant Acetohydroxy Acid Isomeroreductase Homodimer Generates an Active Monomer with Reduced Stability and Altered Magnesium Affinity†

Peter M. Wessel,‡ Valérie Biou,§ Roland Douce,‡ and Renaud Dumas*,‡

Unité Mixte CNRS/Rhône-Poulenc (UMR 41), Rhône-Poulenc Agrochimie, 14-20, rue Pierre Baizet, 69263 Lyon, Cedex 09, France, and Laboratoire de Cristallographie Macromoléculaire, Institut de Biologie Structurale Jean Pierre Ebel, 41 avenue des Martyrs, 38027 Grenoble, France

Received February 20, 1998; Revised Manuscript Received May 28, 1998

ABSTRACT: Plant acetohydroxy acid isomeroreductase is a stable homodimer which catalyzes in the presence of magnesium an alkyl migration followed by a NADPH-dependent reduction. Since the enzyme exhibits no kinetic cooperativity either for its cofactor (NADPH and magnesium) or for its substrates, the reason for dimerization of this enzyme was not obvious. Recently, crystallographic studies [Biou, V., et al. (1997) *EMBO J. 16*, 3405−3415] revealed that the loop of residues 422−431 plays a major part in the dimer interface. To understand the role of the quaternary structure of the enzyme, we have deleted residues 423−430 and substituted Phe 431 for serine. This mutant was further overproduced in *Escherichia coli*, purified to homogeneity, and characterized. Gel filtration and thermodynamic experiments disclosed that this mutant behaves as an active monomer with reduced thermal stability. Furthermore, kinetic and fluorescence experiments showed that the behavior of the monomer with respect to magnesium was greatly altered. These results demonstrate the function of the quaternary structure of plant acetohydroxy acid isomeroreductase in the stabilization of the tertiary structure but also in the stabilization of a high-affinity magnesium binding site.

Acetohydroxy acid isomeroreductase from *Spinacia oleracea* L. (EC 1.1.1.86) forms a stable homodimer with a molecular mass of 114 kDa and one active site per monomeric subunit (*1*, *2*). The enzyme is involved in the biosynthetic pathway of the essential amino acids valine, leucine, and isoleucine. It catalyzes an unusual two-step reaction (Figure 1) consisting of an alkyl migration in which the substrate, either 2-acetolactate (AL)[1] or 2-aceto-2-hydroxybutyrate (AHB), is converted to 3-hydroxy-3-methyl-2-oxobutyrate or 3-hydroxy-3-methyl-2-oxopentanoate, followed by a NADPH-dependent reduction to give 2,3-dihydroxy-3-isovalerate or 2,3-dihydroxy-3-methylvalerate, respectively. The overall reaction has a strong requirement for magnesium with a K_d value of 6 μM (*3*). The enzyme-catalyzed reaction obeys an ordered mechanism in which NADPH and magnesium bind first, followed by acetohydroxy acid substrate binding (*2*, *4*).

Recently, the crystallographic structure of the spinach enzyme complexed with NADPH, magnesium ions, and *N*-hydroxy-*N*-isopropyloxamate (IpOHA, a transition state analogue) revealed details of the enzyme structure and the

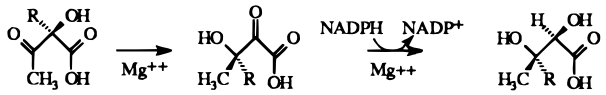

FIGURE 1: Reaction catalyzed by acetohydroxy acid isomeroreductase. The migrating alkyl chain is symbolized with an R, corresponding to CH_3 or CH_2CH_3 for (2*S*)-2-acetolactate (AL) or (2*S*)-2-aceto-2-hydroxybutyrate (AHB), respectively. The reaction products, (2*R*)-2,3-dihydroxy-2-isovalerate and (2,3*R*)-2,3-dihydroxy-3-methylvalerate, are converted to valine and isoleucine, respectively.

geometry of the active site (*5*). The two monomeric subunits of the homodimer are equivalent. Each monomer consists of two structural domains: an α/β N-terminal domain (residues 82−307) involved in the NADPH-binding fold and an all α-helical C-terminal domain (residues 308−595) which interacts with two magnesium ions. The active site region is at the interface between these two domains and is deeply buried inside the protein core. The two magnesium ions, Mg1 and Mg2, interact with two different regions of the C-terminal domain, defined as regions III and IV (*3*, *5*). Mg1 is in direct contact with Asp 315 and Glu 319 from region III, whereas Mg2 is in direct contact with Asp 315 from region III and in indirect contact (via water molecules) with Glu 492 and Glu 496 of region IV. Thus, magnesium Mg2 acts as a bridge between regions III and IV.

In previous works (*3*, *5*), we have demonstrated that the structure of the plant enzyme is very different from those of the bacterial and fungal enzymes. Indeed, although these enzymes catalyze the same reaction, only 24 amino acids are identical in a sequence comparison between plant and

† This study has been conducted under the BioAvenir program financed by Rhône-Poulenc with the contribution of the Ministère de la Recherche et de l'Espace and the Ministère de l'Industrie et du Commerce Extérieur.

* Corresponding author. Fax: 334 72 85 22 97.

‡ Rhône-Poulenc Agrochimie.

§ Institut de Biologie Structurale Jean Pierre Ebel.

[1] Abbreviations: AL, 2-acetolactate; AHB, 2-aceto-2-hydroxybutyrate; IpOHA, *N*-hydroxy-*N*-isopropyloxamate.

S0006-2960(98)00411-5 CCC: $15.00
Published on Web 08/25/1998

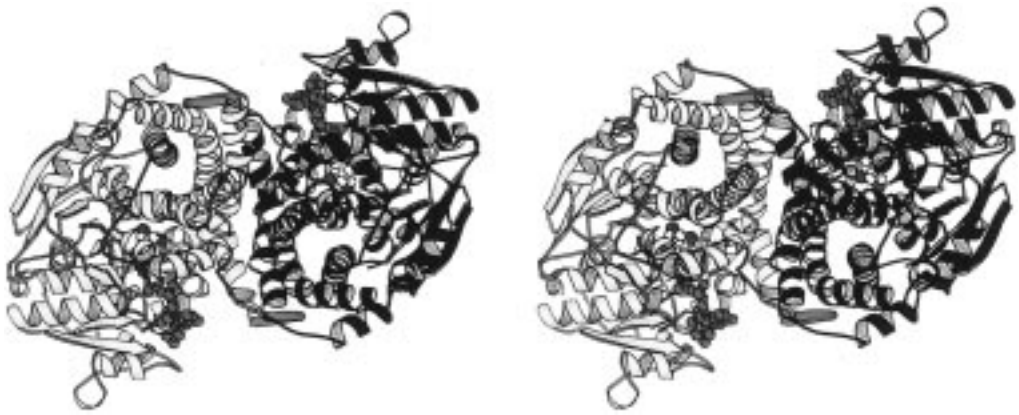

FIGURE 2: Stereoview of a ribbon representation of the spinach acetohydroxy acid isomeroreductase dimer. The positions of the active site and the dimer interface are visible. The deleted part of the loop that extends out toward the other monomer is red. NADPH, inhibitor IpOHA, and magnesium are red, white, and green spheres, respectively. The figure was created using Molscript (*16*).

microorganism acetohydroxy acid isomeroreductases (*3*). Furthermore, whereas in fungi and most bacteria, regions III and region IV are clustered, a supplementary sequence of 140 amino acids belonging to the C-terminal domain exists between the two magnesium binding sites of the plant enzymes (*3*). Interestingly, most of the residues involved in the dimer interface belong to this supplementary sequence. Thus, in addition to playing a function in the formation of the active site and in particular in the binding of the magnesium ions, the C-terminal domain of the plant enzyme is involved in the interactions between the two monomers.

A loop between residues Phe 422 and Phe 431 extends out to the other monomer (Figure 2). It is in contact with surface residues of three α-helices of the other monomer (Tyr 393−Asp 405 of helix A17, Ser 410 of helix A18, and Glu 477−Lys 482 of helix A20) via a number of salt bridges, hydrogen bonds (direct and via water molecules), and hydrophobic interactions (Figure 2) (*5*). Indeed, the interaction between Leu 428 and Ile 478 is the only interface contact which shields hydrophobic side chains. Therefore, this loop can be expected to play an important role in the dimer stabilization of the plant enzyme.

The reason for dimerization of plant acetohydroxy acid isomeroreductase is not obvious. Indeed, the wild-type dimeric acetohydroxy acid isomeroreductase exhibits no kinetic cooperativity either for the substrate (AHB or AL) or for the cofactors (magnesium and NADPH) (*2*, *6*). Furthermore, the investigation of the three-dimensional structure shows that the two active sites of the dimer are equivalent and not constructed directly by the dimer interactions (*5*).

To understand the advantages of dimer fomation for this enzyme, we have constructed a monomeric plant acetohydroxy acid isomeroreductase. Since the subunit interactions are well-known since the investigation of the plant crystal structure (*5*), it seems that the best way to obtain a monomeric enzyme is the selective mutation or deletion of amino acids that are involved in the dimer formation as described for the monomerization of triosephosphate isomerase (*7*). Thus, we have constructed a monomeric acetohydroxy acid isomeroreductase by deletion of the loop of residues 423−430 and substitution of Phe 431 for serine. The kinetic and thermodynamic properties of the obtained monomeric acetohydroxy acid isomeroreductase were further studied.

MATERIALS AND METHODS

Materials. Restriction enzyme endonucleases were supplied by New England Biolabs. IPTG was supplied by Boehringer (Meylan, France) and NADPH by Sigma-Aldrich (Steinheim, Germany). Oligonucleotides used for site-directed mutagenesis and sequencing were obtained from Oligo Express (Paris, France) and Live Technologies (Cergy Pontoise, France).

Strains. *Escherichia coli* strain BMH-71-18 mutS was supplied with the unique site eliminition (USE) mutagenesis kit (Pharmacia) and used during the mutagenesis procedure. Overexpression of proteins was realized in *E. coli* JM 105. The mutagenesis was conducted with plasmid pKK-AHIR that contains the coding sequence for the mature spinach acetohydroxy acid isomeroreductase (*2*).

Site-Directed Mutagenesis. Mutagenesis was carried out using the USE mutagenesis kit (Pharmacia) that utilizes a two-primer system to generate site-specific mutations (*8*). The selection primer 5′-ACGCGCGAGGCGGCCGCGG-TAAAG-3′ is directed to the vector sequence of pKK-AHIR and transforms a unique and nonessential site of a restriction enzyme (*Pvu*II) into another unique restriction site (*Not*I). The mutagenic primer 5′-CGAAGTGTTGTTTTGGCTGG-ACGGCGCTTC*TCTCCAATGGGTAAAATTGATCAA-ACCAGA-3′ is directed to the sequence of the mature spinach cDNA (note that the position of the 24-base deletion is marked by an asterisk and the codon of the F431S mutation is underlined). It carries the desired deletion and/or mutation and effects the loss of a unique *Stu*I site. Identification of positively mutagenized clones was carried out by restriction mapping. The whole sequence of the coding region of the mutagenisated clone has been sequenced by Genome Express SA (Grenoble, France) to ensure no other mutations took place.

Expression and Purification of the Mutant (Δ423−430/F431S) Protein. *E. coli* JM105 cells expressing the pKK-AHIRΔ423−430/F431S plasmid encoding the mutant enzyme were grown at 28 °C in 1 L of LB medium supplemented with streptomycin and carbenicillin (25 and 100 μg/mL, respectively). Isopropyl β-D-thiogalactoside (IPTG) was added to a final concentration of 1 mM when the bacterial growth was equivalent to an A_{600}, of 0.5 and the cells were allowed to continue growing for 15 h at 28

°C. The cells were harvested by centrifugation, and the pellet was resuspended in 7 mL of buffer A [20 mM MOPS (pH 7.5), 1 mM EDTA, 5 mM aminocaproate, 1 mM benzamidine, and 10% glycerol (v/v)] and sonicated by a Vibra-cell disruptor (Sonics and Materials, Danbury, CT). The crude extract was centrifuged at 20000*g* for 30 min to yield a cell-free supernatant. The soluble protein extract (600 mg of protein in 10 mL), which contains the mutant enzyme, was applied to a 25/40 Sephacryl 300 column (Pharmacia) connected to a Pharmacia FPLC system previously equilibrated in 800 mL of buffer A. The enzyme was eluted with 136 mL of buffer A (flow rate of 1 mL/min, fraction size of 2 mL). The chromatographic fractions containing the mutant enzyme (354 mg) were applied to a 16/10 Source Q column (Pharmacia) connected to a Pharmacia FPLC system previously equilibrated with 400 mL of buffer A. Elution was performed with a 300 mL gradient of 0 to 50 mM potassium phosphate (pH 7.5) in buffer A (flow rate of 1 mL/min, fraction size of 1 mL). Chromatographic fractions containing the mutant enzyme were concentrated to 2 mL by centrifugation at 5000*g* in a Macrosep-10 unit (Filtron), previously saturated with 10% glycerol (v/v). This extract (1.4 mg) was then applied to a Hiload 16/60 Superdex 75 column (Pharmacia) connected to a Pharmacia FPLC system previously equilibrated in 200 mL of buffer B [20 mM MOPS (pH 7.5) and 10% glycerol (v/v)]. The enzyme was eluted with 56 mL of buffer B (flow rate of 1 mL/min, fraction size of 1 mL). The chromatographic fractions containing the mutant enzyme (0.9 mg) were concentrated by centrifugation at 5000*g* in a Macrosep-10 unit (Filtron) and stored at −80 °C until they were used. The purity of the mutant protein was analyzed using SDS−PAGE gel stained with Coomassie Brilliant Blue R250. The wild-type enzyme was purified as previously described (*2*). The native masses of the wild-type and mutant enzymes were determined by gel filtration performed on a Hiload 16/60 Superdex 75 column (Pharmacia) under the conditions described above.

Enzyme Assays. Except if otherwise specified, all enzyme activity assays were carried out in a 1 cm optical path length quartz cuvette containing buffer Tris-HCl (50 mM, pH 8.2), $MgCl_2$ (1−3000 μM), and NADPH (3−185 μM) in a final volume of 1 mL at 30 °C. Reactions were usually initiated by adding racemic 2-aceto-2-hydroxybutyrate to a final concentration of 1.3 mM (3.3−2360 μM for measurement of the K_m for AHB), and the process of the reaction was monitored by the decrease in absorbance of NADPH at 340 nm (Uvikon 860 spectrophotometer, Kontron). A ϵ value of 6250 mol^{-1} cm^{-1} was used to calculate the specific activity and the k_{cat} values. Calculations were performed by using the Kaleidagraph program (Abelbeck Software) on a Macintosh computer system. All enzyme concentrations and amounts are given on a per-enzyme-subunit basis.

Fluorescence Studies. Fluorescence measurements were carried out at 460 nm in a SFM 25 (Kontron) fluorimeter, using a 1 mL cuvette and an excitation wavelength of 370 nm at 30 °C as described in a previous study (*3*). The binding of magnesium to the acetohydroxy acid isomeroreductase−NADPH complex was measured using the variations of the emitted fluorescence of the enzyme−NADPH complex upon Mg^{2+} addition. For the wild-type enzyme, the K_d value was determined as previously described (*3*) using a tight binding equation:

$$F_{460}^{exp} = F_0 + \Delta F_{460}^{max} \frac{c_0 + l_0 + K_d - \sqrt{(c_0 + l_0 + K_d)^2 - 4c_0 l_0}}{2c_0} \quad (1)$$

where c_0 and l_0 are the total concentrations of the enzyme−NADPH complex and magnesium, respectively, F_0 is the initial fluorescence, and F_{460}^{max} is the maximum change of fluorescence achieved at saturation.

For the mutant enzyme, the experimental data were analyzed in terms of a complex equilibrium which involves tight binding of a magnesium to a strong affinity binding site (dissociation constant, K_{d1}; maximal fluorescence change, ΔF_{460}^1) and binding of another magnesium to a lower-affinity binding site on the enzyme−NADPH complex (dissociation constant, K_{d2}; maximal fluorescence change, ΔF_{460}^2):

$$F_{460}^{exp} = F_0 + \Delta F_{460}^1 \frac{c_0 + l_0 + K_d - \sqrt{(c_0 + l_0 + K_d)^2 - 4c_0 l_0}}{2c_0} + \Delta F_{460}^2 \frac{l_0}{K_{d2} + l_0} \quad (2)$$

Thermal Activation. The cell jacket of the spectrophotometer was set at different temperatures (7.5−55 °C) by connecting it with a Ministat (Huber, Germany) circulating bath. The 1 cm optical path length quartz cuvette containing 1 mL of buffer Tris-HCl (50 mM, pH 8.2) and $MgCl_2$ (10 mM) was equilibrated to the desired temperature in the spectrophotometer for at least 10 min. NADPH (200 μM) and enzyme (108 nM mutant or 25 nM wild type) were added; the solution was mixed, and after incubation for 10 s, the reaction was initiated by adding racemic 2-aceto-2-hydroxybutyrate to a final concentration of 1.3 mM. Activity data were obtained by analyzing the first 12 s of enzyme activity at reading intervals of 2 s. An Arrhenius plot [log-(k_{cat}) vs $1/T$ (K^{-1})] allows the determination of the reaction activation energy E_a according to equation

$$E_{a\ activation} = -2.303Rm \quad (3)$$

where m is the slope of the Arrhenius plot, 2.303 is the factor of natural log to log, and R (1.987 cal mol^{-1}) is the gas constant

Activation enthalpy values $\Delta H^*_{activation}$ were calculated according to the equation

$$\Delta H^*_{activation} = E_a - RT \quad (4)$$

Activation Gibbs free energy values $\Delta G^*_{activation}$ were calculated according to the equation

$$\Delta G^*_{activation} = -2.303RT \log[(k_{cat}h)/(kT)] \quad (5)$$

where h (1.584×10^{-34} cal s) is Planck's constant and k (3.298×10^{-24} cal K^{-1}) is the Bolzmann constant.

Activation entropy values ΔS^* were then calculated according to the equation

$$\Delta G^*_{activation} = \Delta H^*_{activation} - T\Delta S^*_{activation} \quad (6)$$

Thermal Inactivation. A small volume of enzyme (40 μL) was incubated in a water bath at the desired inactivation temperature. At intervals, an aliquot of enzyme was taken out and quickly added to a cuvette containing 1 mL of buffer Tris-HCl (50 mM, pH 8.2) and $MgCl_2$ (10 mM). The remaining enzyme activity was monitored at a constant temperature of 30 °C for 20 s after adding racemic 2-aceto-2-hydroxybutyrate to a final concentration of 1.3 mM. The constant for thermal inactivation $k_{\text{inactivation}}$ (s^{-1}) is a temperature-dependent time constant of inactivation. The $k_{\text{inactivation}}$ values for the different temperatures are conveniently obtained from the slopes of log(percent remaining activity) versus time plots. The activation energy for thermal inactivation ($E_{\text{a inactivation}}$) was determined from the slope of an Arrhenius plot [log $k_{\text{inactivation}}$ vs $1/T$ (K^{-1})] and is calculated according to eq 3. The activation enthalpy and activation entropy values for thermal inactivation ($\Delta H^*_{\text{inactivation}}$ and $\Delta S^*_{\text{inactivation}}$) are calculated according to eqs 4 and 6, respectively. The activation free Gibbs energies for thermal inactivation, $\Delta G^*_{\text{inactivation}}$, were calculated according to the equation

$$\Delta G^*_{\text{inactivation}} = -2.303RT \log k_{\text{inactivation}} \qquad (7)$$

RESULTS

Choice of the Mutant (Δ423−430/F431S). To investigate the importance of dimer formation in the function of acetohydroxy acid isomeroreductase, we sought to destabilize the dimer. The crystal structure of the enzyme (*5*) showed that the interface resulted from the interactions between antiparallel helices and a 10-residue loop (Phe 422−Phe 431) which extends to the other monomer. This loop by itself accounts for 25% of the total nonbonded interactions in the interface. Therefore, we first tried to delete this loop. Since the distance between the Cα of Phe 422 and the N of Pro 432 is about 4.4 Å, we decided to delete residues 423−430, keeping residue 431 as a linker. Since this residue is a phenylalanine, we mutated it to serine to avoid exposing an apolar residue.

Purification of the Mutant Enzyme. Overproduction and purification of the mutant enzyme as previously described for the wild-type enzyme gave an active enzyme with some degradations. Therefore, the previous procedure was modified to obtain a pure and intact enzyme as shown in Figure 3. The new protocol (see Materials and Methods) includes the use of an amphipathic buffer (20 mM MOPS) and glycerol (10%, v/v). Furthermore, the purification steps were changed. Gel filtration on a Sephacryl S 300 column followed by anion-exchange chromatography on Source Q and gel filtration on Superdex 75 allowed complete purification of the mutant protein (Figure 3 and Table 1). Figure 3 indicates that the eigh-amino acid deletion of the mutant enzyme is visible as a slight difference in migration compared with the wild-type enzyme. The purified mutant, conserved at −80 °C in 20 mM MOPS and 10% glycerol (v/v), is stable for several months without a noticeable loss of activity.

Determination of the Oligomerization State of the Mutant Enzyme. Gel filtration assays were carried out on Superdex S 75 either with the mutant or with the wild-type purified enzymes. When run separately, wild-type and mutant enzymes eluted in a single peak corresponding to elution volumes of 50 and 56 mL, respectively (Figure 4a,b).

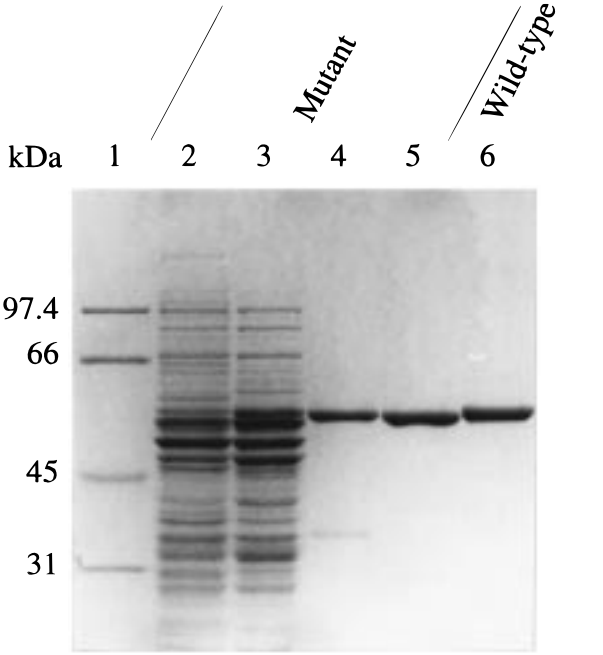

FIGURE 3: Demonstration of the purification procedure for the mutant acetohydroxy acid isomeroreductase by SDS−PAGE. Proteins were separated on a 10% polyacrylamide (w/v) slab gel under denaturating conditions and stained with Coomassie Brillant Blue R250: lane 1, M_r markers; lane 2, soluble proteins of the transformed *E. coli* crude extract, 20 μg; lane 3, Sephacryl 300 pool, 20 μg; lane 4, Source Q pool, 5 μg; lane 5, Superdex 75 pool, 5 μg; and lane 6, purified wild-type enzyme, 5 μg. Note that the eight-amino acid deletion of the mutant enzyme is visible as a slight difference in migration compared with that of the wild-type enzyme.

Therefore, the mutant eluted as a monomeric enzyme with a molecular mass of 60 kDa, and the wild-type enzyme eluted as a dimeric form with a molecular mass of 110 kDa. As shown in Figure 4b, no equilibrium exists between the monomer and the dimeric form. Furthermore, rechromatography of the monomeric enzyme (up to 25 nmol) on Superdex S 75 gives only a monomer, demonstrating that the monomer does not reassociate. Even in the presence of magnesium (3 mM) in the elution buffer, the mutant enzyme eluted as a monomeric enzyme (not shown). Figure 4c also indicates that the monomeric enzyme exhibits an activity lower (of ca. 25%) than that determined for the wild-type enzyme.

Thermodynamics of Activation and Inactivation for the Monomeric and Dimeric Enzyme. The specific activity of the dimeric and monomeric enzymes exhibits strong differences with respect to temperature (Figure 5). First, the specific activity of the monomeric enzyme is lower than that of the wild-type enzyme (3.8 times lower at 30 °C) (see also Figure 4c). Second, denaturation of the monomeric enzyme occurs at temperatures lower (35 °C) than those required to inactivate the dimeric enzyme. Finally, from the Arrhenius plot shown in Figure 5, the thermodynamic constants for activation $E_{\text{a activation}}$, $\Delta H^*_{\text{activation}}$, $\Delta G^*_{\text{activation}}$, and $\Delta S^*_{\text{activation}}$ have been determined for both the mutant and the wild-type enzyme (Table 2). These results essentially demonstrate that the monomer needs more energy ($E_{\text{a activation}} = 20.59 \pm 0.20$ kcal mol^{-1}) to catalyze the reaction compared to the dimer ($E_{\text{a activation}} = 11.03 \pm 0.50$ kcal mol^{-1}).

Moreover, rate constants ($k_{\text{inactivation}}$) of thermal inactivation of the monomer exhibit strong differences compared to those

Table 1: Purification Procedure for the Mutant Acetohydroxy Acid Isomeroreductase from Spinach Overexpressed in *E. coli*[a]

purification stage	total protein (mg)	total activity (μmol of NADPH oxidized min^{-1})	specific activity (μmol of NADPH oxidized min^{-1} mg^{-1})	yield (%)
crude extract of soluble proteins	645	19.4	0.03	100
Hiload 25/40 Sephacryl 300 pool	354	14.4	0.04	74
Hiload 16/10 Source Q pool	1.4	3.2	2.3	16
Hiload 16/60 Superdex 75 pool	0.9	2.7	3.0	14

[a] The total protein was determined with the Bio-Rad protein assay during purification steps or by detection at 205 nm for the pure enzyme. The enzyme activity was mesured at 30 °C in Tris-HCl standard buffer (pH 8.2) with 10 mM $MgCl_2$, 200 μM NADPH, and 1.3 mM 2-aceto-2-hydroxybutyrate.

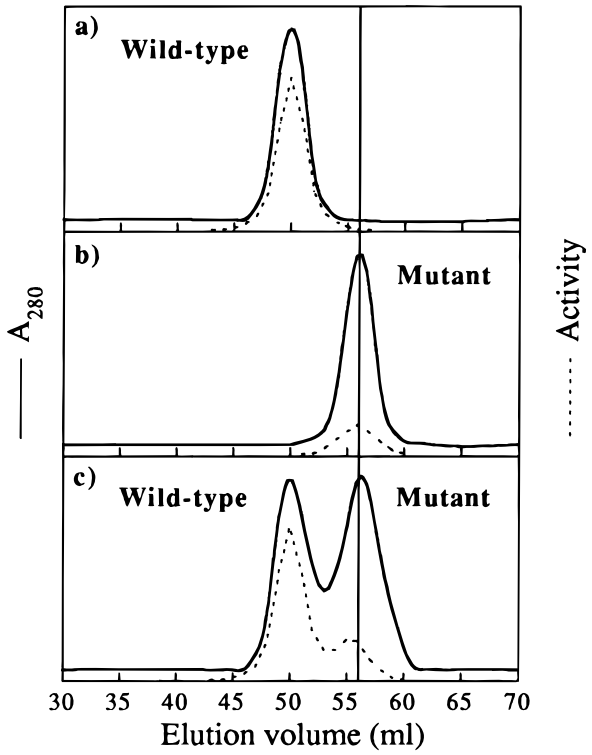

FIGURE 4: Gel filtration profiles of wild-type and mutant acetohydroxy acid isomeroreductase. The elution profile (solid lines) is shown as well as the measured enzyme activity (dotted lines). Panels a and b show the elution profiles for the wild-type (5 nmol) and the mutant enzyme (5 nmol) run separately; in panel c, a mixture of equal amounts of wild-type and mutant enzyme (5 nmol each) was injected. The wild-type enzyme elutes at 50 mL, corresponding to a homodimer with a molecular mass of 110 kDa (calculated mass of 114 kDa). The mutant enzyme elutes at 56 mL, corresponding to a monomeric enzyme with a molecular mass of 60 kDa (calculated mass of 55 kDa).

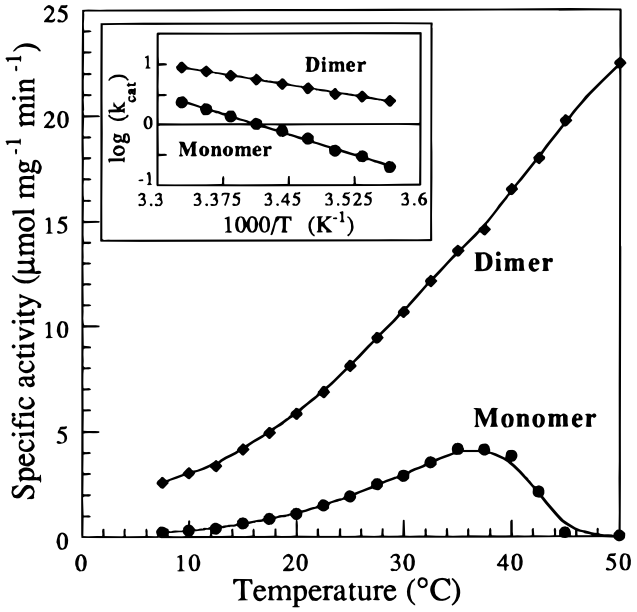

FIGURE 5: Temperature dependence of enzyme activity for wild-type and mutant acetohydroxy acid isomeroreductase (see Table 1). A quartz cuvette containing the standard reaction buffer was equilibrated in a cell jacket set to the desired temperature. The enzyme (25 nM wild-type or 108 nM mutant) was added in a small volume (5 μL); the solution was mixed quickly, and the reaction was started by adding 1.3 mM AHB. The enzyme activity was monitored by the decrease of NADPH absorbance at 340 nm for 20 s. The inset shows an Arrhenius plot for the thermal activation. Log(k_{cat}) values for wild-type and mutant enzymes are plotted vs the reciprocal temperature. The calculated E_a values are 11.03 $\pm$ 0.20 and 20.59 $\pm$ 0.50 kcal mol^{-1} for the dimeric wild-type and the monomeric mutant, respectively (eq 3).

Table 2: Thermal Activation Parameters[a]

	wild-type enzyme	mutant enzyme
$E_{a\ activation}$ (kcal mol^{-1})	11.03 $\pm$ 0.20	20.59 $\pm$ 0.50
$\Delta H^*_{activation}$ (kcal mol^{-1})	10.44 $\pm$ 0.20	20.00 $\pm$ 0.50
$\Delta G^*_{activation}$ (kcal mol^{-1})	16.25 $\pm$ 0.02	17.12 $\pm$ 0.02
$\Delta S^*_{activation}$ (cal mol^{-1} K^{-1})	$-$19.49 $\pm$ 0.78	9.66 $\pm$ 1.76

[a] Thermal activation parameters ΔH^*, ΔG^*, and ΔS^* were calculated for a temperature of 25 °C as described in Materials and Methods, using the Kaleidagraph program (Abelbeck Software) on a Macintosh computer system.

of the dimer (Figure 6). From the Arrhenius plots (log $k_{inactivation}$ vs 1/T, not shown) deduced from Figure 6, the thermodynamic constants for inactivation $E_{a\ inactivation}$, $\Delta H^*_{inactivation}$, $\Delta G^*_{inactivation}$, and $\Delta S^*_{inactivation}$ have been determined for both the mutant and the wild-type enzyme (Table 3). These results essentially show that ΔG^* for thermal inactivation reached negative values at a lower temperature for the monomer (47 °C) than for the dimer (54 °C), demonstrating that thermal denaturation occurs at a lower temperature for the monomer than for the dimer.

Steady State Kinetic Properties. Kinetic experiments for both the wild-type and the mutant enzyme were carried out at 30 °C in the standard reaction buffer using AHB as the substrate. The rate plot of v (steady state rate of NADPH oxidation) versus concentration of the mutant enzyme is linear in the range of 0−275 pmol of monomer (not shown), evidence of adherence to steady state conditions. To understand the effect of enzyme monomerization on the

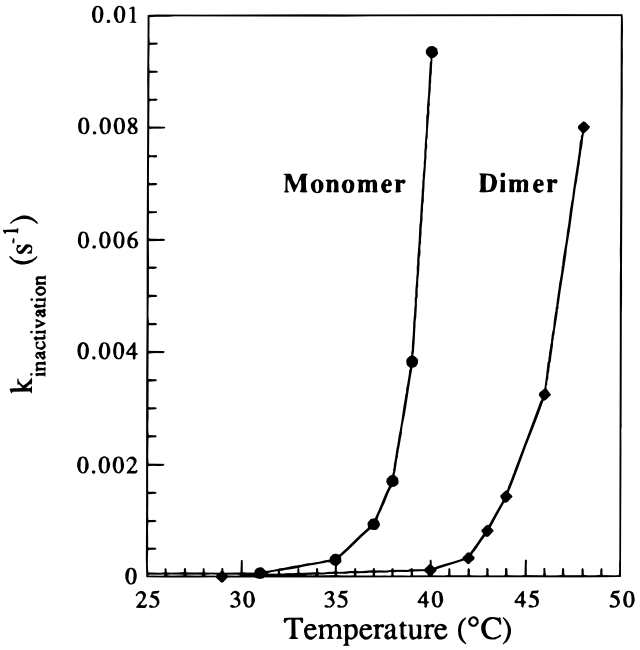

FIGURE 6: Thermostability of the wild-type dimer and mutant monomer acetohydroxy acid isomeroreductase (see Table 2). The heat inactivation rate constants ($k_{inactivation}$) for the wild-type dimer and mutant monomer are plotted against the inactivation temperature. The heat inactivation rate constants were obtained from the slopes of log(remaining activity) plotted against inactivation time. The enzyme [18 μM in 40 μL of purification buffer B [20 mM MOPS (pH 7.5) and 10% glycerol (v/v)]] was inactivated at different temperatures. At time intervals, small aliquots were taken out and quickly added to a quarz cuvette containing the standard reaction buffer (at 30 °C) and the solution was mixed. The reaction was started by adding 1.3 mM AHB, and the enzyme activity was monitored by the decrease of NADPH absorbance at 340 nm.

Table 3: Thermal Inactivation Parameters[a]

	wild-type enzyme	mutant enzyme
$E_{a\ inactivation}$ (kcal mol^{-1})	113.23 ± 8.25	118.72 ± 7.42
$\Delta H^*_{inactivation}$ (kcal mol^{-1})	112.63 ± 8.25	118.12 ± 7.42
$\Delta G^*_{inactivation}$ (kcal mol^{-1})	10.83 ± 0.80	8.69 ± 0.55
$\Delta S^*_{inactivation}$ (cal mol^{-1} K^{-1})	341.40 ± 30.39	367.05 ± 26.27
$\Delta G^*_{inactivation}$	0 at 54 °C	0 at 47 °C

[a] Thermal inactivation parameters ΔH^*, ΔG^*, and ΔS^* were calculated for a temperature of 25 °C as described in Materials and Methods, using the Kaleidagraph program (Abelbeck Software) on a Macintosh computer system. The temperature needed to reach a ΔG^* value of 0 was also determined.

NADPH and magnesium binding sites, the K_m values of the monomer for NADPH and magnesium ions were determined, respectively.

The K_m value of the mutant enzyme for NADPH (5.2 μM) does not differ considerably from that obtained for the wild-type enzyme (3.5 μM), indicating that the NADPH binding site of the monomer and the dimer should be similar.

However, as observed in Figure 7, magnesium affinity has been dramatically altered by monomerization. As previously determined (*2*), Figure 7 shows that despite the existence of two magnesium ions in the active site, the dimeric wild-type enzyme exhibits perfect Michaelis−Menten behavior, indicating that the two magnesium binding sites of each monomer are equivalent. In marked contrast, the monomeric mutant enzyme shows strong cooperative properties against magnesium with a Hill coefficient of 1.9 (Figure 7). This

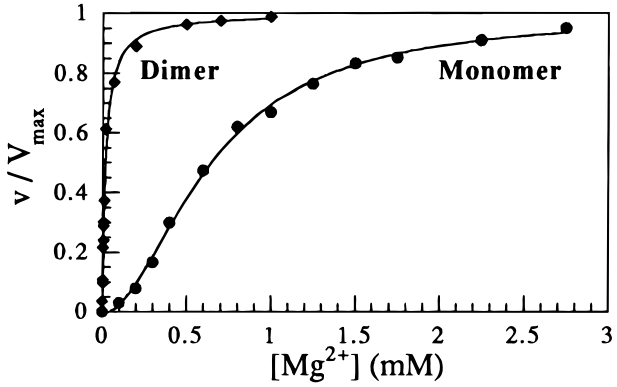

FIGURE 7: Magnesium dependence of activity for the wild-type dimer and mutant monomer acetohydroxy acid isomeroreductase. v/V_{max} is plotted against the magnesium concentration. While magnesium fixation of the wild-type enzyme corresponds perfectly to Michaelien kinetics with a K_m of 10 μM, the two magnesium sites of the monomeric mutant enzyme exhibit strong cooperativity with a binding constant of 640 μM and a Hill coefficient of 1.9.

latter result shows that the monomer binds at least two magnesium ions. This result suggests also that the magnesium binding sites of the monomeric enzyme are no more equivalent. Furthermore, the observed positive cooperativity may indicate that binding of a first magnesium in one of the magnesium binding sites facilitates a second magnesium to bind on a vacant site. Figure 7 also indicates that the monomerization of the enzyme leads to a decrease in magnesium affinity, since the concentration of magnesium needed to reach the half-maximum velocity increases from 10 to 640 μM between the dimer and the monomer. As noted above, the kinetic cooperativity was not due to a shift from the monomeric to dimeric enzyme upon raising the Mg^{2+} concentration since gel filtration experiments demonstrated that the mutant enzyme retained a monomeric conformation even in the presence of magnesium.

Subsequent determination of the K_m value for the substrate AHB at saturated concentrations of magnesium and NADPH allows us to see if upon fixation of the cofactors the conformation of the active site of the monomer−NADPH−Mg^{2+} complex is similar to that of the dimer−NADPH−Mg^{2+} complex. It appears that the K_m value of the monomer for racemic AHB (53 μM) is quite similar to that determined for the wild-type enzyme (20 μM). In addition, the investigation of the effect of the inhibitor IpOHA on the mutant enzyme disclosed that this compound behaves as a slow and tight binding competitive inhibitor of the monomeric enzyme (not shown) as previously demonstrated for the wild-type enzyme (*9*). Our results demonstrate, therefore, that upon fixation of NADPH and magnesium ions, the overall conformations of the active site of the monomeric and dimeric enzyme should be quite similar.

Fluorescence Studies. Binding of magnesium to the wild type and to the monomeric acetohydroxy acid isomeroreductase was also assessed directly by fluorescence measurements (Figure 8). As previously described for the wild-type enzyme (*2*), there is a marked enhancement of NADPH fluorescence in the presence of the wild-type or the mutant enzyme, an indication of the formation of a binary complex between NADPH and these enzymes. When magnesium was added to the wild type−NADPH binary complex, the plot of emitted fluorescence as a function of the concentration

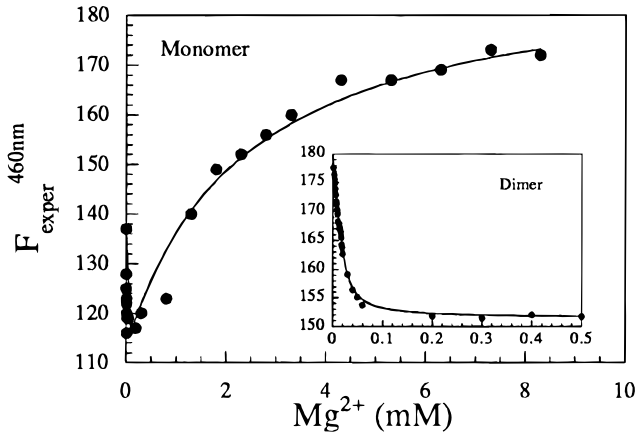

FIGURE 8: Fluorimetric characterization of the interaction between mutant acetohydroxy acid isomeroreductase and Mg^{2+}. Assays were carried out in 200 μL of 50 mM Tris-HCl (pH 8.2) containing 65 μM NADPH and 14 μM enzyme. The excitation wavelength was 370 nm, and the emission wavelength was 460 nm. After stepwise addition of Mg^{2+} (0.2 μL additions of different Mg^{2+} stock solutions), the emitted fluorescence was recorded. The data were fitted using eq 2 (see Materials and Methods) assuming the binding of a first magnesium (K_d = 10 μM) on a site with a high affinity and the binding of a second magnesium (K_d = 2300 μM) on a site with a low affinity. The inset shows the plot of emited fluorescence determined with the wild-type enzyme. The data were analyzed on the basis of a tight binding hypothesis (K_d = 6 μM) using eq 1 (see Materials and Methods).

of added Mg^{2+} decreases in a single-exponential curve defining a site of high affinity with a K_d value for Mg^{2+} of 6 μM (Figure 8), as previously determined with the dimeric enzyme (*3*). Therefore, consistent with kinetic measurements, this result indicates that the two magnesium binding sites of each subunit are equivalent. However, when magnesium was added to the mutant−NADPH binary complex, the plot of emitted fluorescence as a function of the concentration of added Mg^{2+} exhibited two saturation curves. A first decreasing curve defining a site with a high affinity for the metal ion with a K_d value of 10 μM was followed by a second increasing curve defining a second binding site with a lower affinity for the metal ion and exhibiting a K_d value of 2300 μM. Therefore, these results demonstrate that monomerization of the enzyme generated a magnesium binding site with a low affinity. Furthermore, consistent with kinetic studies, these results show that the magnesium binding sites of the monomer are no more equivalent.

DISCUSSION

Oligomerization is common for a wide range of proteins (*10*). As 70−80% of all enzymes are oligomeric and only about 32% of these exhibit kinetic cooperativity (*11*), the advantage of oligomerization for many enzymes is not a priori obvious. Several studies characterizing monomeric subunits of oligomeric enzymes show that besides cooperativity, three general advantages result from oligomerization such as folding of the oligomeric protein (*12*, *13*), formation and stabilization of the active sites of monomeric subunits, or maintaining the stability of the tertiary structure (*14*, *15*).

To understand the function of dimerization in plant acetohydroxy acid isomeroreductase, we have generated an active monomer of plant acetohydroxy acid isomeroreductase by deleting residues between Phe 422 and Phe 431 and substituting Phe 431 by serine.

In the wild-type dimeric enzyme, the residue Ile 428 shields hydrophobic contact with Ile 478 of the other monomer. However, the crystallographic model shows that the hydrophobic side chain of Ile 478 is also located in a hydrophobic pocket in the same monomer and would not be totaly exposed to the solvent in the monomeric enzyme. Consistent with this finding, further mutation of Ile 478 of the monomeric enzyme to alanine, serine, or threonine increased the instability of the monomer (not shown). Therefore, we decided to keep Ile 478 for the production of the monomeric enzyme.

The purified monomer does not reassociate into a dimer since rechromatography of the mutant (up to 25 nmol) on Superdex 75 led to a monomeric enzyme. Furthermore, since the rate plot of v (steady state rate of NADPH oxidation) versus concentration of the mutant enzyme is linear in the range of 0−275 pmol of monomer, this further suggests that the aggregation state of the mutant enzyme is independent of its concentration.

This study on acetohydroxy acid isomeroreductase indicates that monomerization of the plant acetohydroxy acid isomeroreductase leads to a 4-fold decrease in specific activity, to a decrease of thermal stability, and at least to strong modifications of magnesium affinity. These results give us new insights into the function of the plant acetohydroxy acid isomeroreductase quaternary structure. Indeed, the dimerization clearly stabilizes the tertiary structure since it protects the enzyme against thermal denaturation. Also, the dimerization has an important function in the stabilizing of the active site since both specific activity and magnesium affinity have been altered.

The X-ray structure showed that the wild-type enzyme has two magnesium binding sites (*5*). Furthermore, previous biochemical works on mutants affected by the binding of these two ions demonstrated that the two magnesium ions are required for the catalytic reaction (*3*). The fact that the monomer is still active suggests that the monomer still binds two magnesium ions. Furthermore, kinetic (Figure 7) and fluorescent (Figure 8) experiments carried out with magnesium demonstrate that the monomer has at least two different magnesium binding sites. To account for these results, one possible hypothesis is that monomerization generated a third magnesium binding site with a low affinity, which would be involved in the reaction. However, a more simple and rational hypothesis is that the stoichiometry of maximal magnesium binding in the monomer has not been altered and that monomerization induced a decrease in affinity for one of the two magnesium binding sites. Interestingly, the fluorimetric behavior of the monomer is similar to that observed with a region IV mutant E488D affected by the binding of magnesium Mg2 (*3*). Our fluorescence experiments carried out on the purified monomer suggest, therefore, that the two observed saturation curves may correspond to the fixation of magnesium Mg1 on a site with a high affinity (region III) followed by the binding of magnesium Mg2 on a site with a lower affinity (between regions III and IV). In addition, the observed kinetic cooperativity of magnesium suggests that primary binding of magnesium Mg1 on region III may somewhat stabilize the binding site of magnesium Mg2, allowing the binding of magnesium Mg2. Thus, the

strong decrease in magnesium affinity, the modification of the Michaelis−Menten behavior to a cooperative behavior, and the change in the fluorescence properties are particularly important in understanding the function of quaternary structure of the plant acetohydroxy acid isomeroreductase. It is clear, therefore, that the plant acetohydroxy acid isomeroreductase quaternary structure plays a role in the stabilization of a magnesium binding site with a high affinity.

Despite the alteration of the binding site of magnesium Mg2 induced by monomerization, we have shown that the affinity of the monomeric enzyme for NADPH is similar to those observed for the dimeric wild-type enzyme. Thus, it appears that monomerization does not induce conformational change or destabilization at the level of the N-terminal NADPH domain. Such a result can be easily understood in terms of previous crystallographic work demonstrating that dimeric interactions do not involve the N-terminal domain but occur only at the level of the C-terminal domain of each monomer. Furthermore, it appears that the conformation of the monomer active site upon binding of NADPH and magnesium ions should also be similar to those of the dimer complexed with NADPH and magnesium ions. Indeed, both the K_m for AHB and the behavior with IpOHA are similar for the monomeric and dimeric enzymes. These results therefore demonstrate that the active sites of the dimer and the monomer do not have the same conformation before binding of the two magnesium ions but become similar after binding of the two cations.

To determine the modifications of conformation occurring at the level of the active site of the monomeric enzyme, we are currently studying the mutant and the wild-type enzyme with proton−deuterium exchanges and mass spectrometry experiments. Also, the crystallization of the monomeric enzyme is in progress.

ACKNOWLEDGMENT

We are grateful to Gilles Curien, Fréderic Halgand, Dominique Job, and Prof. Elmar W. Weiler for helpful comments.

REFERENCES

1. Dumas, R., Lebrun, M., and Douce, R. (1991) *Biochem. J. 277*, 469−475.
2. Dumas, R., Job, D., Ortholand, J. Y., Emeric, G., Greiner, A., and Douce, R. (1992) *Biochem. J. 288*, 865−874.
3. Dumas, R., Butikofer, M. C., Job, D., and Douce, R. (1995) *Biochemistry 34*, 6026−6036.
4. Chunduru, S. K., Mrachko, G. T., and Calvo, K. C. (1989) *Biochemistry 28*, 486−493.
5. Biou, V., Dumas, R., Cohen-Addad, C., Douce, R., Job, D., and Pebay-Peyroula, E. (1997) *EMBO J. 16*, 3405−3415.
6. Dumas, R., Joyard, J., and Douce, R. (1989) *Biochem. J. 262*, 971−976.
7. Borchert, T. V., Abagyan, R., Jaenicke, R., and Wierenga, R. K. (1994) *Proc. Natl. Acad. Sci. U.S.A. 91*, 1515−1518.
8. Deng, W. P., and Nickoloff, J. A. (1992) *Anal. Biochem. 200*, 881−976.
9. Dumas, R., Cornillon-Bertrand, C., Guigue-Talet, P., Genix, P., Douce, R., and Job, D. (1994) *Biochem. J. 301*, 813−820.
10. Janin, J., Miller, S., and Chotia, C. (1988) *J. Mol. Biol. 204*, 155−164.
11. Traut, T. W. (1994) *Crit. Rev. Biochem. Mol. Biol. 29*, 125−163.
12. Grant, G. A., Al-Rabiee, R., Xu, X. L., and Zhang, Y. (1997) *Biochemistry 36*, 3353−3358.
13. Shao, X., Hensley, P., and Matthews, R. (1997) *Biochemistry 36*, 9941−9949.
14. Beernink, P. T., and Tolan, D. R. (1996) *Proc. Natl. Acad. Sci. U.S.A. 93*, 5374−5379.
15. Schliebs, W., Thanki, N., Jaenicke, R., and Wieranga, K. (1997) *Biochemistry 36*, 9655−9662.
16. Kraulis, P. J. (1991) *J. Appl. Crystallogr. 24*, 946−950.

BI980411G